

## Estimation of the chemical composition in the "knee" region from the muon/electron ratio in EAS

**The KASCADE Collaboration** : T. Antoni<sup>1</sup>, W.D. Apel<sup>1</sup>, F. Badea<sup>2</sup>, K. Bekk<sup>1</sup>, K. Bernlöhner<sup>1</sup>, E. Bollmann<sup>1</sup>, H. Bozdog<sup>2</sup>, I.M. Brăncuș<sup>2</sup>, A. Chilingarian<sup>4</sup>, K. Daumiller<sup>5</sup>, P. Doll<sup>1</sup>, J. Engler<sup>1</sup>, F. Fessler<sup>1</sup>, H.J. Gils<sup>1</sup>, R. Glasstetter<sup>5</sup>, R. Haeusler<sup>1</sup>, W. Hafemann<sup>1</sup>, A. Haungs<sup>1</sup>, D. Heck<sup>1</sup>, J.R. Hörandel<sup>1</sup>, T. Holst<sup>1</sup>, K.-H. Kampert<sup>5</sup>, H. Keim<sup>1</sup>, J. Kempa<sup>6</sup>, H.O. Klages<sup>1</sup>, J. Knapp<sup>5</sup>, H. Leibrock<sup>1</sup>, H.J. Mathes<sup>1</sup>, H.J. Mayer<sup>1</sup>, J. Milke<sup>1</sup>, D. Mühlenberg<sup>1</sup>, J. Oehlschläger<sup>1</sup>, M. Petcu<sup>2</sup>, H. Rebel<sup>1</sup>, M. Risse<sup>1</sup>, M. Roth<sup>1</sup>, G. Schatz<sup>1</sup>, H. Schieler<sup>1</sup>, F.K. Schmidt<sup>5</sup>, T. Thouw<sup>1</sup>, H. Ulrich<sup>1</sup>, J. Unger<sup>1</sup>, B. Vulpescu<sup>2</sup>, J.H. Weber<sup>1</sup>, J. Wentz<sup>1</sup>, T. Wibig<sup>6</sup>, T. Wiegert<sup>1</sup>, D. Wochele<sup>1</sup>, J. Wochele<sup>1</sup>, J. Zabierowski<sup>7</sup>, S. Zagromski<sup>1</sup>.

<sup>1</sup> Forschungszentrum Karlsruhe, Institut für Kernphysik, D 76021 Karlsruhe, Germany; <sup>2</sup> Institute of Physics and Nuclear Engineering, RO 7690 Bucharest, Romania; <sup>3</sup> Physikalisches Institut, Univ. Tübingen, D 72076 Tübingen, Germany; <sup>4</sup> Cosmic Ray Division, Yerevan Physics Institute, Yerevan 36, Armenia; <sup>5</sup> Institut für Experimentelle Kernphysik, Univ. Karlsruhe, Germany; <sup>6</sup> Department of Experimental Physics, Univ. Lodz, PL 90950 Lodz, Poland; <sup>7</sup> Szoltan Institute for Nuclear Studies, PL 90950 Lodz, Poland

New data on the muon/electron ratio derived from the KASCADE extensive air shower experiment are presented. This ratio is known to be the most sensitive parameter in the determination of the mass of the primary particle when using ground array data. The particle numbers are measured with the KASCADE array comprising 500 m<sup>2</sup> of e/γ- and 620 m<sup>2</sup> of μ- detectors. The primary mass is inferred on an event-by-event basis by comparing the experimental data to corresponding EAS simulations. We observe a change towards a heavier composition with increasing energy above the knee. The sensitivity of this result to the specific hadronic interaction model employed in the simulations (e.g. VENUS and QGSJET) is discussed.

### 1. Experimental setup and observables

The KASCADE detector array measures the lateral electron and muon distributions in extensive air showers. One aim is to obtain the electron and muon numbers that give important clues to mass and energy of the primary particle. The array comprises about 500 m<sup>2</sup> of e/γ- and 620 m<sup>2</sup> of μ- detectors which are housed in 252 detector stations and are arranged in a grid of 200 x 200 m<sup>2</sup> size. They are described in more detail elsewhere ([1]). The muon detectors are positioned directly below the e/γ- detectors and are shielded by slabs of lead and iron corresponding to 20 radiation lengths in total. This imposes an energy threshold of about 300 MeV to muons. Because of the geometrical arrangement many muons will deposit energy in the e/γ- detector before entering the muon detector. On the other hand, energetic photons or electrons may penetrate the shielding,

thereby faking a muon signal. Hadrons will also deposit energy in both types of detectors. These effects were corrected for by an iterative method using the energy deposits in the detectors and applying results of simulations. The mutual deposits of electrons, photons and hadrons in the e/γ- and μ- detectors were obtained by extensive simulations with the CORSIKA event generator [2] taking into account the response of the KASCADE experiment. The simulation data set produced includes different primary masses and zenith angles and covers a wide energy range. With these simulations lateral energy correction functions were calculated to convert energy deposits to particle numbers.

## 2. Determination of electron and muon numbers.

Data processing and shower analysis is performed in a three-step procedure. In a first step the shower core and shower direction are reconstructed to apply the lateral correction functions and to convert the energy deposits to particles. A rough estimation for the electron and muon numbers is done by parametrisation of the total energy deposits. After iterative corrections for electromagnetic punch through in the  $\mu$ -detectors and the muonic energy deposit in the  $e/\gamma$ -detectors the electron and muon densities are both fitted by NKG-functions. The electrons are fitted with a radius parameter of 89 m, the muon fit function uses a fixed slope parameter, calculated from electron number and zenith angle, and a radius parameter of 420 m in a fit range of 40–200 m. The lower radius cut is due to uncertainties of hadronic and electromagnetic punch through, that may deposit even more energy than the muons at distances close to the shower core. The upper cut reflects the limits of geometrical acceptance. In a final level a subsequent NKG fit using the muon distribution as a background function provides the final electron number and lateral distribution. This fitted function is used to correct the energy deposits in the  $\mu$ -detectors. The muon densities are then fitted with a NKG function again. By integrating this function from zero to infinity, we obtain the muon size  $N_\mu$ . Alternatively, an integration within the range of the fits gives the truncated muon size  $N_\mu^{tr}$ , which is approximately a factor of 4 smaller than the total muon size. This observable has the advantage to be free of systematical errors caused by extrapolations outside the experimental acceptance. The systematic uncertainty of the reconstructed particle numbers is about 5% and is well understood. The reconstruction accuracy is dominated by sampling fluctuations and is about 5% for the electron size and 10% for the muon size at the knee.

## 3. Estimation of composition from the muon/electron ratio.

The data presented here were taken out of  $\sim 6 \cdot 10^7$  reconstructed showers. The following principal cuts were applied to the reconstructed events in order to ensure reliable reconstruction results:

The reconstructed shower core was within a radius of 91 m from the center of the array and the accepted shower age was restricted to  $0.2 \leq \text{age} \leq 2$ . An energy threshold of approximately  $10^{15}$  eV guarantees 100% trigger and reconstruction efficiency for proton and iron showers. The data were subdivided into narrow zenith angle bins. The zenith angle of the data shown in Figure 1 and Figure 2 was restricted to  $18^\circ \leq \theta \leq 26^\circ$ . About 580.000 showers survived these cuts. In the following the data were subdivided into 8 energy bins ( $9 \cdot 10^{14} \text{ eV} \leq E_0 \leq 10^{16} \text{ eV}$ ), that were calculated by the simulated correlations of electron and muon numbers to the primary energy. The binning calculated with VENUS differs slightly from the binning calculated with the QGSJET model. The simulated data consist of three mass groups: light masses (represented by protons and helium), medium masses (oxygen) and heavy masses (iron). 5000 showers were produced for each of the elements with an energy slope of  $E^{-1}$ . These showers were finally analysed with the reconstruction code used for the raw data and given a weight of  $E^{-1.7}$  to be comparable with data.

A four-parameter maximum likelihood fit was performed to the muon/electron ratio distributions within these bins. The fit function was given by the sum of the four simulated element distributions which were approximated by Gaussians. The fitted parameters are the weights of these distributions. The results for helium and proton were added to give the weight of the light group. Figure 1 and 2 demonstrate the quality of the fit for two energy bins ( $6.25 \leq \log_{10}(E_0/\text{GeV}) \leq 6.4$  and  $6.55 \leq \log_{10}(E_0/\text{GeV}) \leq 6.7$ ).

The different results of the fit as shown in figure 2 are mainly due to larger shower fluctuations predicted by the QGSJET model.

The experimental data can be described reason-

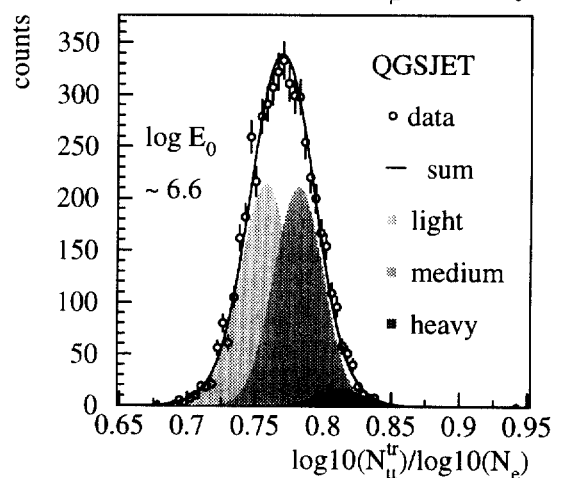
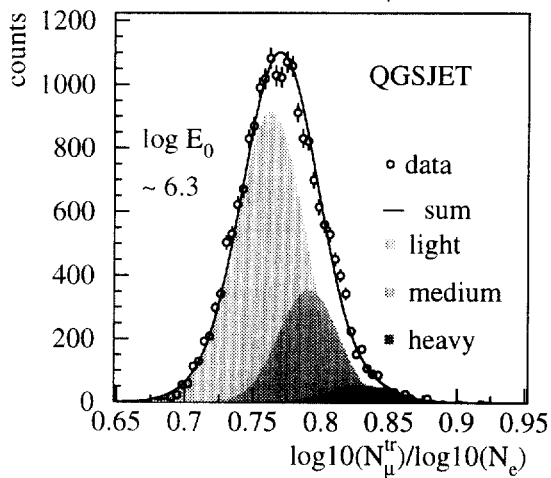
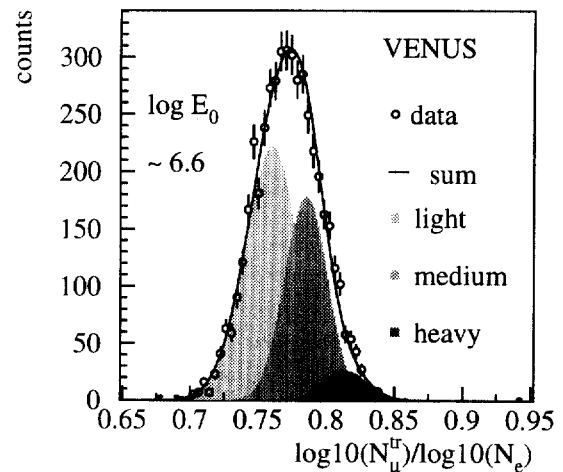
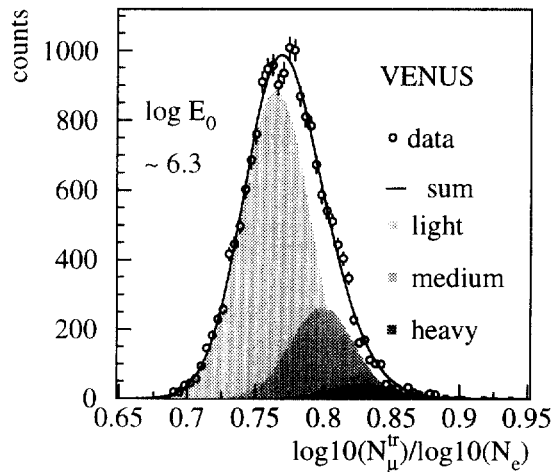


Figure 1. The muon/electron ratio distributions for an energy at  $\sim 2 \cdot 10^{15}$  eV

Figure 2. The muon/electron ratio distributions for an energy at  $\sim 4 \cdot 10^{15}$  eV

ably well by both VENUS and QGSJET simulations. The simulations show no severe shift to the left or the right side of the data distribution. Figure 3 a) shows the fit results for all 8 bins for the VENUS prediction: A mild trend to a lighter composition up to the knee and then an increasing part of the medium and heavy masses can be observed. The energy region where the composition changes significantly corresponds to the knee position in the electron size spectra analysed by [3]. Using the QGSJET model (Figure 3 b) the behaviour below the knee looks qualita-

tively similar to the VENUS results, but there is an enhancement of medium mass above the knee position. The lowest energy bin may be affected by efficiency effects.

A fit to the simulated showers that have been used for the parametrisation of the Gaussian functions shows no systematical error when using a constant composition as input. The careful study of the appropriate parametrisation of the simulated distributions and resulting systematic errors will be continued.

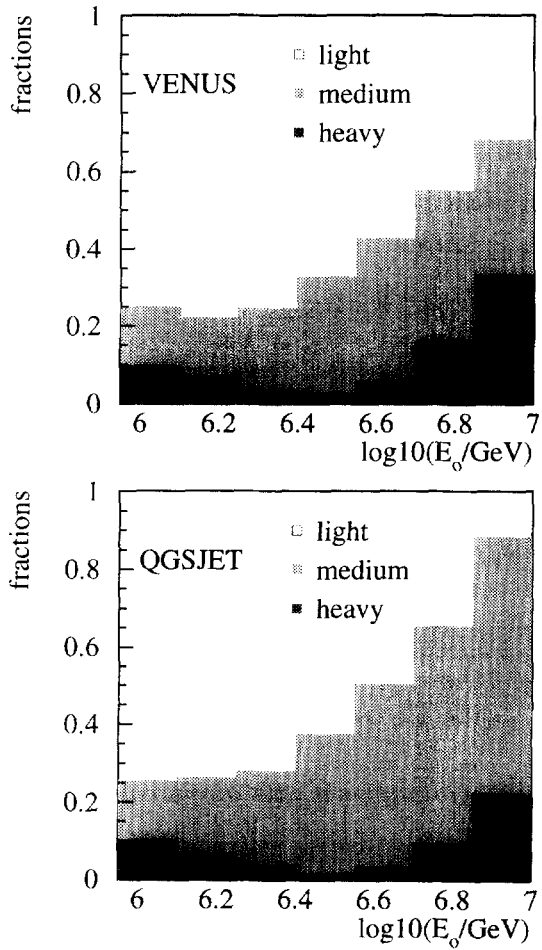


Figure 3. The fractions of the three mass groups as function of primary energy

## REFERENCES

1. H.O. Klages et al., *Nucl. Phys. B (Proc. Suppl.)* 52B (1997) 92
2. Heck, J. Knapp et al., FZKA 6019 Forschungszentrum Karlsruhe (1998)
3. R. Glasstetter et al., *25th ICRC.* (1997) 157–160